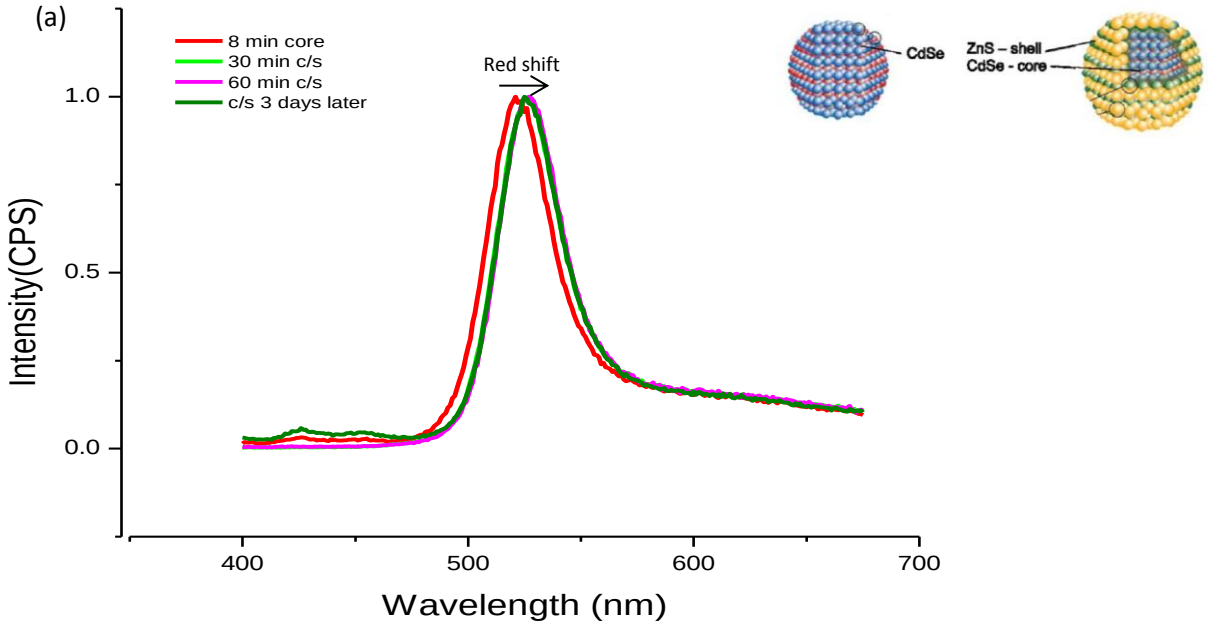

Figure 2.2. PL spectra), CdSe/ZnS core-shell QDs after 30 min (*light green* QDs after 60 min (*pink*) and CdSe/ZnS core-shell QI *green*). The inset shows a schematic diagram of C nd after coating with ZnS (Angell, 2011).

UNIVERSITY of the WESTERN CAPE

No significant differences were observed between the 30 min and 60 min ZnS coating time points. However, a red shift in the emission wavelength from the core to core-shell structure (*green and pink peaks*) was observed. This suggests that an increase in particle size occurred, and therefore, successful ZnS coating of CdSe QDs was achieved as similarly reported (Dabbousi *et al*., 1997 & Pechstedt *et al*., 2010).

The narrow and sharp PL peaks depicted that both the CdSe core and CdSe/ZnS core-shell QDs had a narrow size distribution. Additionally, literature suggests that the surface passivation of the CdSe core with a ZnS coating should result in a higher quantum yield by approximately 50 % (Dabbousi *et al*., 1997). QDs with smaller diameters usually have very large surface-to-volume ratios and the presence of surfactants such as TOP are subjected to broad deep trap emissions as a result of incomplete surface passivation (Dabbousi *et al*., 1997

& Jones *et al*., 2003). The ZnS coating should therefore function as a suppressor of these trap emissions by passivation of the surface trap sites within the crystalline structure (Dabbousi *et al*., 1997). This in turn produces a PL subjected to band-edge recombination and thus, higher quantum yield (Jones *et al*., 2003).

It is important to note the wavelengths at which these particles emit light. Green fluorescent molecules have emission profiles near 500 nm (Bruchez *et al*., 1998). The CdSe/ZnS core/shell QDs emitted light with a wavelength of ~525 nm, as described in **Section 2.4.1.**

.

2.5.2.3. Transmission electron microscopy

To directly investigate the size distribution and morphology of QDs, TEM or HR-TEM may be employed. For biological applications, the importance of producing QDs with particular structural properties would facilitate the ease of functionalising the nanoparticles with biomolecule counterparts (Zhang and Clapp, 2011).

The HR-TEM micrograph for the CdSe/ZnS core-shell QDs is shown in **Figure 2.3**. The micrograph shows that the QDs are relatively monodispersed and spherical in shape. The **inset of Figure 2.3** demonstrates that poor lattice fringes were resolved, revealing that the structural quality of the QDs were not of high quality. This may be as a result of high lattice mismatches between the core and shell materials during the growth phase (Qi, 2001 & Zeng *et al*., 2009).

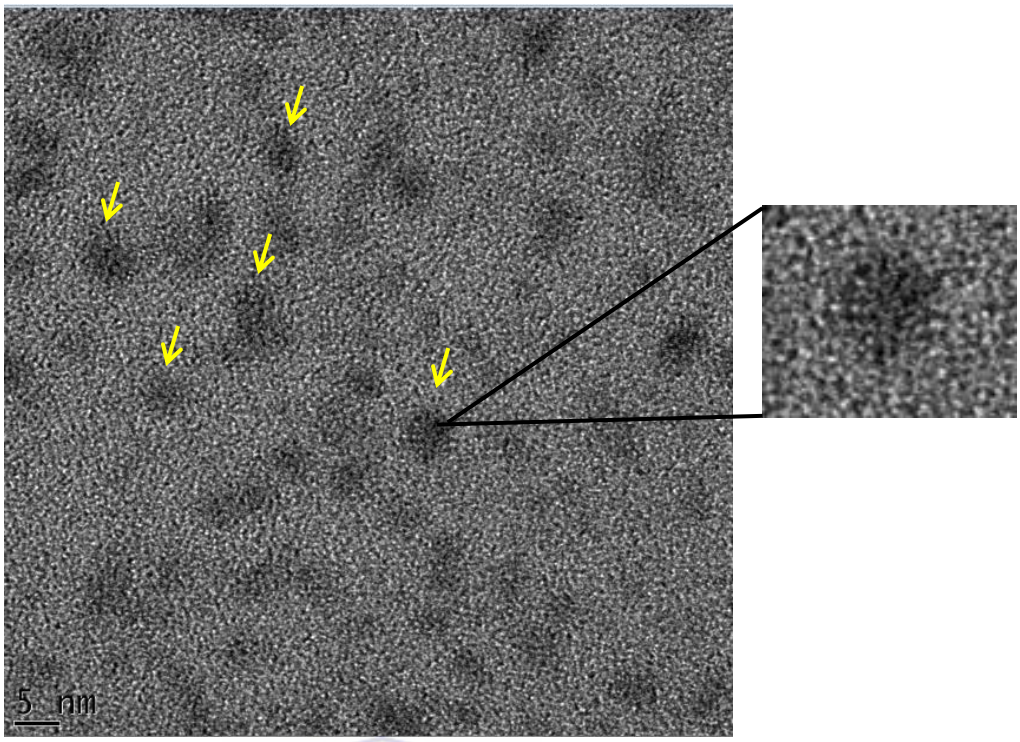

Figure 2.3. High Resolution-TEM micrograph of CdSe/ZnS core-shell QDs.

2.5.2.4. EDS

Physical characterisation of nanomaterials may be achieved at different levels. To confirm the composition of the QDs prepared, the EDS analysis was carried out. The EDS spectrum showed the presence of all the four elements, Cd, Se, Zn and S (**Figure 2.4**).

After successful characterisation by PL spectroscopy, HR-TEM and EDS, it was demonstrated that nearly monodispersed and green fluorescent CdSe/ZnS core-shell QDs were synthesised using an organometallic approach. The results obtained were satisfactory proven to proceed with ligand exchange to solubilise the QDs for a biological environment.

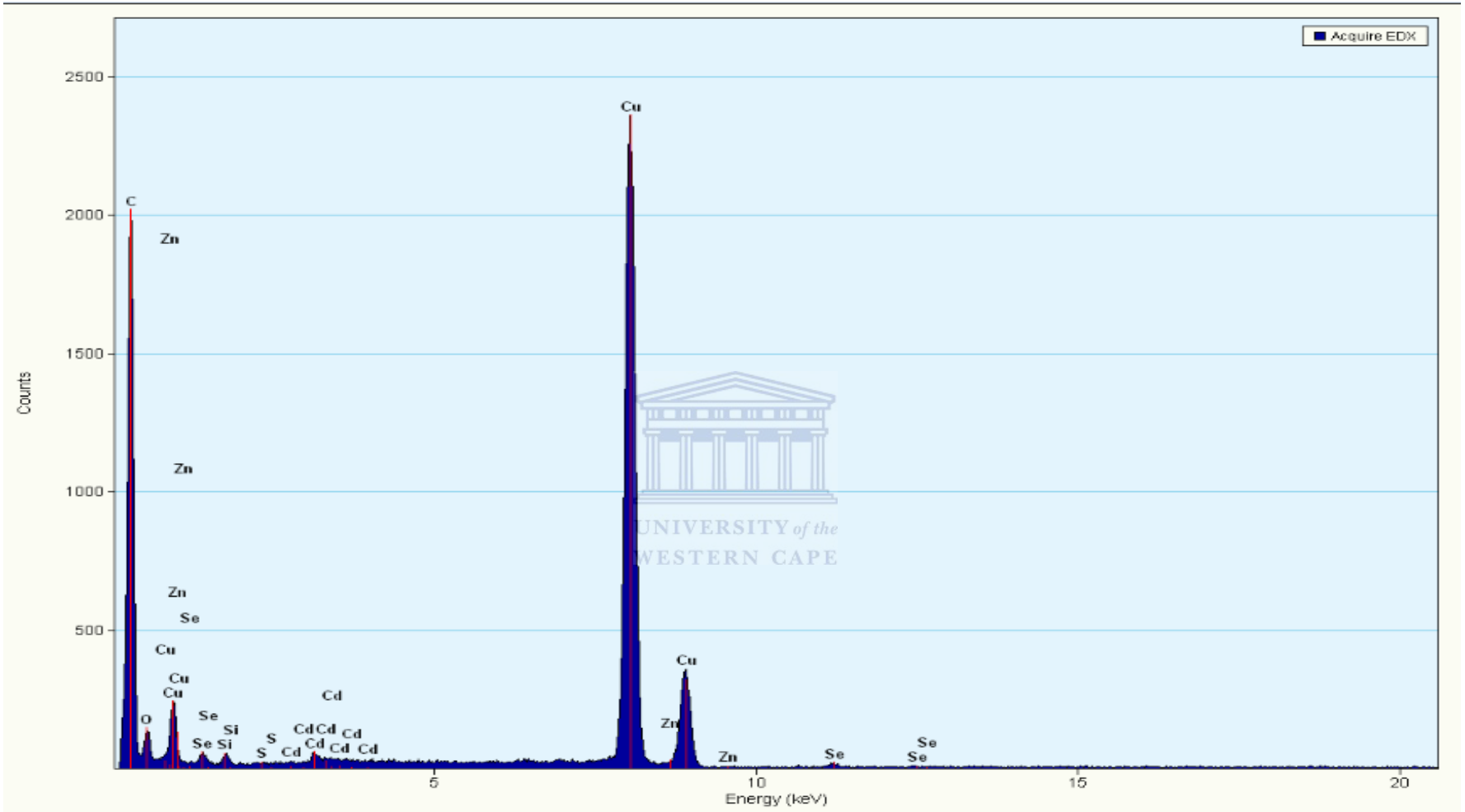

Figure 2.4. EDS spectrum of the as prepared CdSe/ZnS core-shell QDs.

2.6. Water soluble CdSe/ZnS core-shell QDs

2.6.1. Introduction

The organometallic approach produces QDs stabilised by hydrophobic surfactants and therefore an important step is then to ensure that these QDs are rendered water-soluble. This may be achieved by surface modification with hydrophilic or ampiphilic moieties that would facilitate its application in a biological environment (Zhang and Clapp, 2011). The high-temperature synthesis lack intrinsic aqueous solubility, subsequently; phase-transfer to an aqueous solution is required through one of two strategies, that is, encapsulation or ligand exchange. Encapsulation relies on hydrophobic adsorption onto the TOP capped QDs, whereas; ligand exchange relies on mass action by means of heterobifunctional ligands that serve to displace the hydrophobic surfactant. Examples of such ligands include 3-mercaptopropionic acid or L-cysteine, whose carboxyl and amine moieties, respectively, renders the QD water-soluble (Medintz *et al*., 2005)

2.6.2. Ligand Exchange

Ligand exchange approaches reported for L-cysteine capped CdSe/ZnS QDs (Cys-QD) generally involved transferring the QDs from the organic phase to the aqueous phase as described above, however, the resultant Cys-QDs were only stable for 24 hours. Precipitated Cys-QDs were observed as macroscopic aggregates formed as a result of cysteine oxidation, consequently forming cysteine dimers (cystine) that are incapable of binding to the QD surface (Liu *et al*., 2007). An alternative capping strategy proposed by Carrillo-Carrion *et al*., produced bio-compatible and more stably dispersed Cys-QDs which showed a decline in

fluorescence intensity after 2 days, though the dispersion was stable for at least a month (Carrillo-Carrion *et al*., 2009).

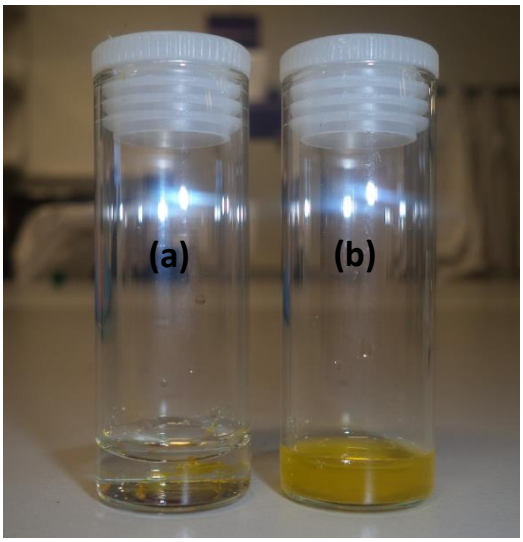

Figure 2.5. Ligand exchange using L-Cysteine (a) CdSe/ZnS core-shell QDs before sonication and (b) after sonication

Figure 2.5 shows the development of water-soluble Cys-QDs using the method described by Carrillo-Carrion *et al*., described in **Section 2.4.3.** Prior to sonication, the TOP capped CdSe/ZnS core-shell QDs remained in its pelleted form, clearly demonstrating the hydrophobicity. However, after sonication (ligand exchange), the Cys-QDs appear well dispersed in the aqueous solution, indicative of a successful ligand exchange. The water-soluble QDs produced in this section were of satisfactory quality to proceed with biological application, when characteristically compared to those discussed above by Carrillo-Carrion *et al*., 2009.

Chapter Three: Selective eradication of cancer cells using peptide directed QDs to deliver a pro-apoptotic peptide

3.1. Introduction

The efficiency of any cancer treatment is directly related to and measured by its capacity to reduce or eradicate tumours and minimally, if at all damage healthy tissue (Byrne *et al*., 2008). Considering this, the therapeutic goal of cancer is to selectively target and kill cancerous cells (Haglund *et al*., 2009 & Sioud and Mobergslien, 2012 & Thundimadathil, 2012). Conventional chemotherapeutic drugs lack the aforementioned ability as a result of non-specific distribution of the drug. Consequently, giving rise to dose-related systematic toxicities, thereby, restricting the amount of drug to be administered and in turn leading to inadequate therapeutic effects (Allen and Cullis, 2004 & Wang *et al*., 2009). For this reason, an alternative strategy is required. Nanoparticle delivery systems offer an improved alternative due to their ability to interact at the cellular level with a great degree of specificity (Byrne et al., 2008 & Singh and Lilard, 2009).

3.2. Objective of this chapter

The objective of this chapter was to, respectively, bi-conjugate the commercially available amino Qdot525 (Qdot525) and the previously synthesised Cys-QDs (Chapter 2) to the LTVSPWY (p.L) and Smac peptides. Then carry out a comparative study to relate the efficiency of the Cys-QDs to the Qdot525 by evaluating whether the respective QD peptide bi-conjugates (Qdot525/p.L+Smac or Cys-QD/p.L+Smac) selectively target and eradicate cancer cells.

3.3. Materials and suppliers

2X Trypsin	Life Technologies
Amino Qdot®525 ITK™	Life Technologies
BM cyclin	Roche
Boric acid	Sigma-Aldrich
Dimethyl sulfoxide (DMSO)	Sigma-Aldrich
Dulbecco's Modified Eagles Media (DMEM)	Whitehead Scientific
1-ethyl-3-(3-dimethylaminopropyl) carbodiimide) (EDC)	Sigma-Aldrich
Ethanol	Merck
Fetal Bovine Serum (FBS)	Biochrome
Fluoroshield with DAPI	Sigma-Aldrich
LTVSPWY peptide	Anaspec
N-acetyl-D-erytho-spinghosine (C2 Ceramide)	Sigma-Aldrich
Nucblue Live Cell Stain	Life Technologies
Paraformaldehyde	Sigma-Aldrich
Penicillin/streptomycin	Whitehead Scientific
PD-10 purification column	GE Healthcare
Phosphate buffered saline (PBS)	Whitehead Scientific
Smac/DIABLO peptide	Anaspec
Sodium Hydroxide	Merck
Triton X-100	Sigma-Aldrich

3.4. Solutions and buffers

3% Bovine Serum Albumin (BSA): 0.3 g/ml BSA was prepared in PBS.

3.5. Methods

3.5.1. Cell culture

HT29 and HeLa cells were cultured in Dulbecco's Modified Eagles Medium (DMEM), supplemented with 10 % penicillin/streptomycin (Life Technologies) and 10 % Fetal Bovine Serum (FBS) (Biochrome).

3.5.2. Thawing of cells

Vials containing the frozen cells were removed from the -150 ^{o}C freezer and allowed to thaw at room temperature. Cells were then transferred to a 15 ml tube containing 3 ml DMEM and the latter transferred into a 25 cm^2 tissue culture flask. The flask was placed in a water jacketed CO_2 incubator (Labotec) at 37 ^{o}C and 5 % CO_2 until 60-90 % confluency was reached.

3.5.3. Trypsinization of cells

Once the cells reached the desired confluency, trypsinization was carried out as follows:

The DMEM in the flask was decanted. Thereafter, the cells were washed with 1 X Phosphate buffered saline (PBS). The PBS was then discarded and the cells were trypsinized with the addition of 1 X trypsin and incubated in a water jacketed CO_2 incubator at 37 ^{o}C for 2-3 min. DMEM was added to the cells to inactivate the trypsin. Cells were collected by centrifugation at 3000 x *g*.

3.5.4. Freezing of cells

Once the cells reached the desired confluency, the cells were removed by trypsinization as described above in **Section 3.5.3**. The cell pellet generated from trypsinization was prepared for long-term storage. The cell pellet was resuspended in DMEM containing 10 % DMSO, and aliquoted into 2 ml cryo-vials and stored at -150 ^{o}C.

3.6. Dose response curves

3.6.1. Seeding of cells

HT29 cells were cultured and trypsinized as described in **Section 3.5.1 and 3.5.3**. The cells were counted using the Countess Automated Cell Counter (Invitrogen). The cells were seeded in to 96-well cell culture plates at a cell density of $1x10^5$ cells/ml. The 96-well cell culture plates were placed into a water jacketed CO_2 incubator at 37 ^{o}C for 24 hrs.

3.6.2. QD Treatment

After 24hrs of culturing, the cells were treated with varying concentrations of QDdot525 (Invitrogen) or Cys-QD (Chapter 2) for 24 hrs in a water jacketed CO_2 incubator at 37 ^{o}C. The treatments were performed in triplicate. After the 24 hrs treatment, the WST-1 Cell Proliferation Reagent (10 µl/well) was added to the respective wells. The cells were further incubated in a water jacketed CO_2 incubator at 37 ^{o}C. The 96-well cell culture plates were agitated for 1 min and absorbance readings were obtained at 440 nm and 620 nm using a Spectrophotometer (BMG labotec).

3.7. Bi-conjugation of QDs to peptides

The reagents as listed in **Tables 3.1 and 3.2**, were added to a clean amber (light protective) glass vial. The reaction mixture was vortexed for 2 hrs at room temperature. Two other

conjugations were setup in a similar manner, in the absence of the Smac peptide and used as controls. The QD peptide bi-conjugates generated from this reaction were: (1) Qdot525/p.L+Smac, (2) Qdot525/p.L, (3) Cys-QD/p.L+Smac and (4) Cys-QD/p.L.

Table 3.1. Bi-conjugation of the Qdot525 to the p.L and Smac peptides

Qdot525/p.L+Smac	Qdot525/p.L	Stock concentration	Final concentration
Borate Buffer (pH 8.5)	Borate Buffer (pH 8.5)	50mM	50 mM
Amino-Qdot525	Amino-Qdot525	8 µM	0.25 µM
p.L peptide	p.L peptide	11595 µM	50 µM
Smac peptide	-	10602 µM	50 µM
EDC	EDC	50 µM	0.375 µM

Table 3.2. Bi-conjugation of the Cys-QD to the p.L and Smac peptides

Cys-QD/p.L+Smac	Cys-QD/p.L	Stock concentration	Final concentration
Borate Buffer (pH 8.5)	Borate Buffer (pH 8.5)	50mM	50 mM
Cys-QD	Cys-QD	14400 µg/ml	350 µg/ml
p.L peptide	p.L peptide	11595 µM	50 µM
Smac peptide	-	10602 µM	50 µM
EDC	EDC	50 µM	0.375 µM

3.8. Desalting of the QD peptide bi-conjugates by gel filtration

The bi-conjugates were subjected to purification using the PD10 desalting column (GE Healthcare) according to the manufacturer's instructions:

The cap at the bottom of the column was removed and the column storage solution was poured off. The sealed end of the column was cut off. The column was then equilibrated by addition of the equilibration buffer (Borate buffer, pH 8.5). The buffer was allowed to migrate into the column bed and the flow through was discarded. This was repeated four

times. The QD-peptide bi-conjugates were added to the respective columns. The QD-peptide bi-conjugates were allowed to migrate into the column bed. The volume was adjusted to 2.5 ml, by addition of the equilibration buffer. The buffer was then allowed to migrate into the column bed. The flow through was discarded. Clean glass vials were placed under the columns for sample collection. The bi-conjugates were collected by addition of the elution buffer (1 X PBS, pH 7.4) at 1000 µl elutes. Aliquots of 100 µl were placed into PCR tubes. An aliquot (100 µl) of the unconjugated QD samples (Qdot525 and Cys-QDs) were included as controls. Images were captured under UV-light (UVP) and the desalted bi-conjugates were stored at 4 ^{o}C until further use.

3.9. Immunocytochemistry

3.9.1. Seeding of cells

HT29 and HeLa cells were cultured and trypsinized as described in **Section 3.5.1 and 3.5.3**. The cells were counted using the Countess Automated Cell Counter (Invitrogen). The cells were seeded onto sterilised coverslips in 6-well cell culture plates at a cell density of 2 x 10^5 cells/ml. The 6-well cell culture plate was placed in a water jacketed CO_2 incubator at 37 ^{o}C and the cells cultured until 50 – 60 % confluency.

3.9.2. Fixation and permeabilisation

Once the cells reached the desired confluency, the media was removed from the cells in 6-well cell culture plates using a pipette. The cells were washed twice with 1 X PBS. The PBS was then discarded and 4 % formaldehyde was added to each well and left for 20 min at room temperature to allow cells to fix to the coverslips. The PBS was then discarded and 0.1 % Triton X-100 was added to each well and left for 5 min to allow permeabilisation of the cell membrane. This was followed by washing the cells twice with 1 X PBS.

3.9.3. Fixed cell staining

The washed cells were then incubated with the respective QD peptide bi-conjugates: Qdot525/p.L+Smac, (2) Qdot525/p.L, (3) Cys-QD/p.L+Smac and (4) Cys-QD/p.L for 1 hr at room temperature. A drop of Fluoroshield DAPI mounting media (Sigma-Aldrich) was placed onto labelled microscope slides. The cells were washed 3 times with PBS and dried by blotting the edges of the coverslip on paper towel. The coverslips were transferred onto the mounting media with the cell-side faced down. The images were captured at 100 X magnification under oil immersion using the fluorescent Carl Zeiss LSM 780 Confocal microscope with Elyra S.1 super resolution platform (Carl Zeiss).

3.9.4. Live cell staining

Cells were seeded as described in **Section 3.9.1**. Once the cells reached the desired confluency, the media was removed from cells in 6-well cells culture plates using a serological pipette. The cells were washed twice with 1 X PBS. The PBS was then discarded and the cells were incubated with the respective QD peptide bi-conjugate for 24 hrs in a water jacketed CO_2 incubator at 37 ^{o}C. The staining medium was then removed using serological pipette and the cells were washed four times with 1 X PBS. The cells were then fixed as described in **Section 3.9.2.** A drop of Nucblue Live Cell Stain was placed onto labelled microscope slides and the cells were mounted and visualised as described in **Section 3.9.3.**

3.10. Cytotoxicity assay

HT29 and HeLa cells were seeded as described in **Section 3.9.1.** After 24 hrs of culturing, the cells were treated with the respective QD peptide bi-conjugates (**Section 3.7**) in the presence or absence of ceramide (60 µM) for 24 hrs in a water jacketed CO_2 incubator at 37 ^{o}C. The treatments were performed in triplicate. After the 24 hr treatment, WST-1 Cell Proliferation

Reagent (10 µl/well) was added to the respective wells. The cells were further incubated for 2 hrs in a water jacketed CO_2 incubator at 37 ^{o}C. The 96-well cell culture plates were agitated for 1 min and analysed using a spectrophotometer (BMG labotec).

3.11. Results and Discussion

3.11.1. Dose response curves to determine optimal QD concentration

To determine a good response model for the drug delivery system, a non-hazardous dosage of the QDs must be obtained. Therefore using a dose response curve, the lethal concentration at ~50 % (LD_{50}) of the QDs and the appropriate, non-hazardous concentration of the QDs required for application in the QD peptide bi-conjugate can be extrapolated. Since the aim of the targeted drug delivery system developed in this study is to sensitise the cells to treatment with ceramide, it is important to ensure that the QDs do not induce toxicity. To accomplish this, HT29 cells were seeded and treated as described in **Sections 3.6.1 and 3.6.2. Figure 3.1** shows the dose response curves for HT29 cells after the 24 hr treatment.

Cellular viability was assessed using the WST-1 Cell Proliferation (Roche) colometric assay. **Figure 3.1** illustrates that a decrease in cell viability is directly proportional to an increase in QD concentration for both the Qdot525 and the Cys-QDs. The LD_{50} values obtained were ~0.8 µM and ~720 µg/ml for Qdot525 and Cys-QDs, respectively. Based on this dose response curve, it was decided to use a concentration below the LD_{50}, 0.25 µM and 350 µg/ml for the Qdot525 and Cys-QDs, respectively.

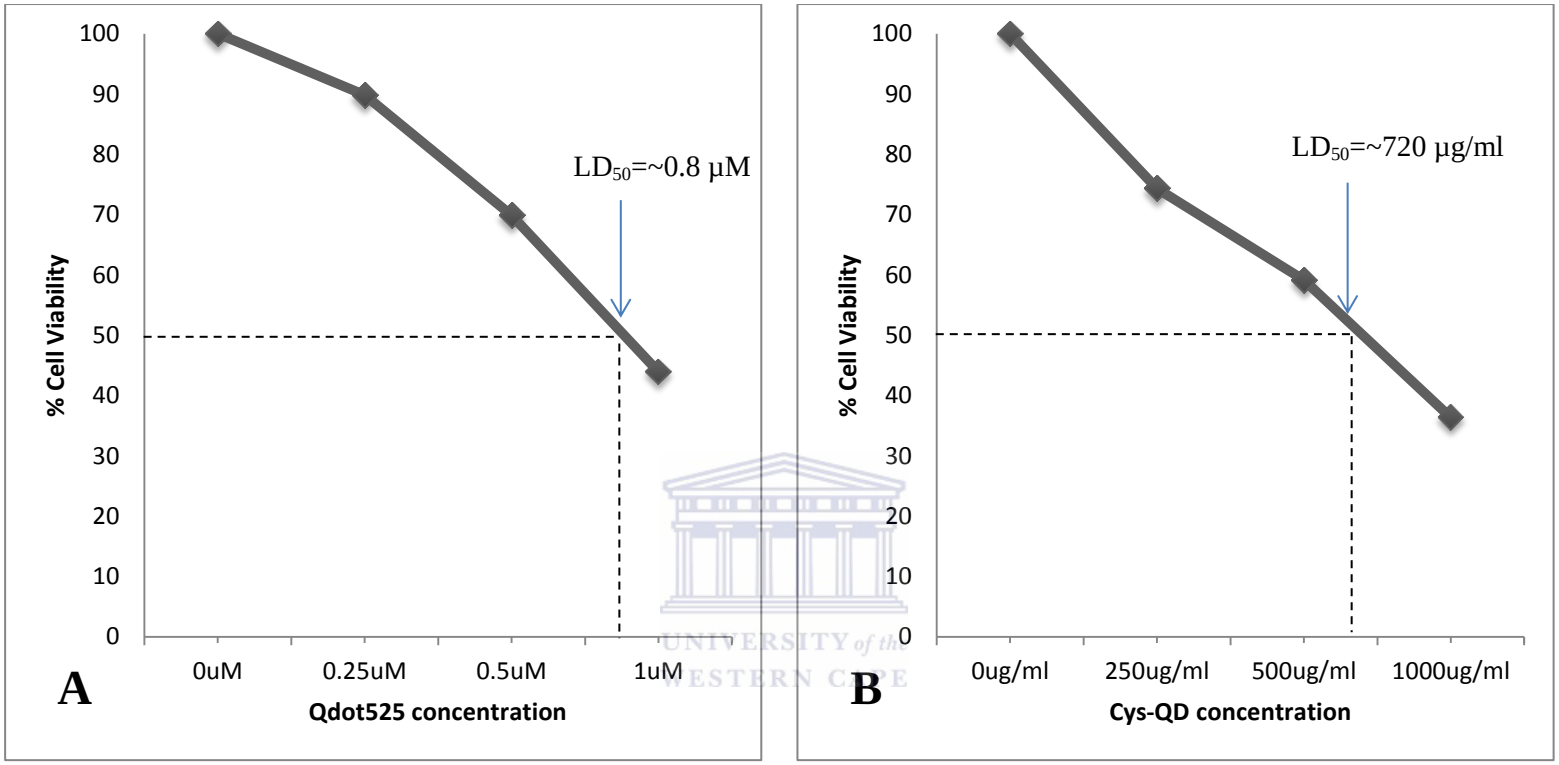

Figure 3.1. Dose response curve of the Qdot525 (A) and Cys-QDs (B). HT29 cells were subjected to treatment with the Qdot525 or the Cys-QD for 24 hrs. Subsequently, the cell viability was determined using the WST-1 Cell Proliferation colometric assay. The data was obtained in triplicate and used to construct dose response curves for the respective QDs (mean ± SD; n=3).

3.11.2. Bi-conjugation of QDs to peptides using EDC chemistry

The specificity of a nanoparticle-based drug delivery system can be achieved by cancer specific peptides; owing to its high-affinity sequences that are easy to conjugate to its' counterparts. Furthermore, its' small size that permits a good degree of tissue penetrability and drug carrying capacity, negligible immunogenicity; and a considerable level of in vivo stability (Jaracz *et al*., 2005 & Li and Cho, 2012). In order to facilitate the use of a drug delivery system, the respective moieties are required to be chemically linked (Hermanson, 2013). EDC is cross-linker most often employed to mediate the bi-conjugation of amino and carboxylate groups (Zhang and Clapp, 2011 & Vashist, 2012).

The objective of this section was to generate four bi-conjugates, namely, (1) Qdot525/p.L+Smac, (2) Qdot525/p.L, (3) Cys-QD/p.L+Smac and (4) Cys-QD/p.L. This was achieved using EDC chemistry as described in **Section 3.6** and schematically illustrated in **Figure 3.2.**

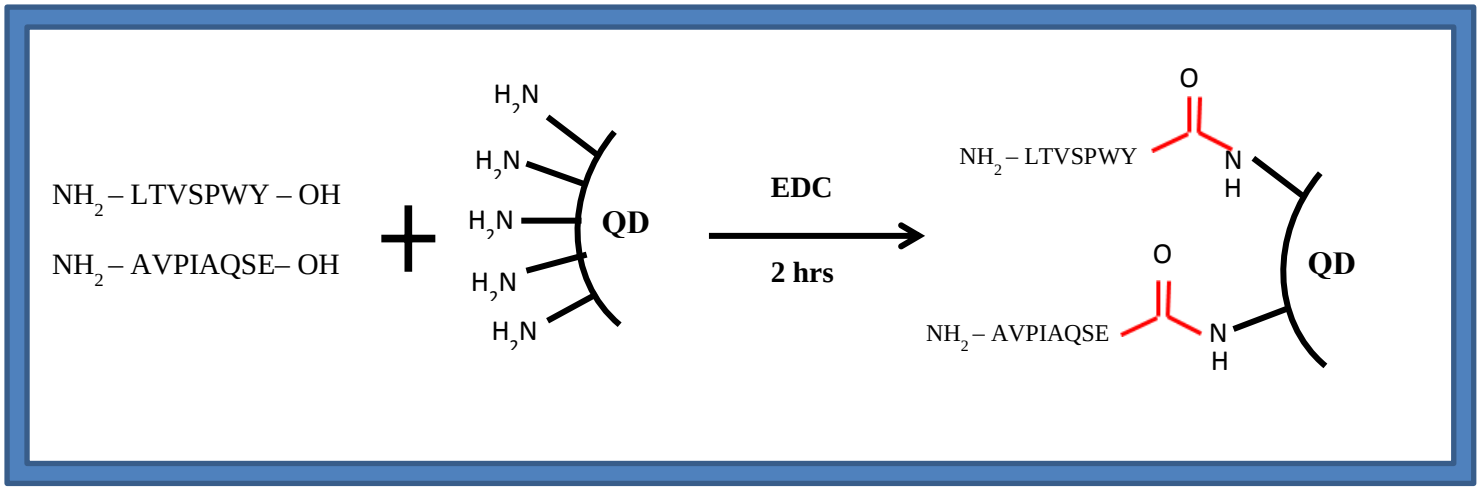

Figure 3.2. Schematic diagram illustrating cross-linking of amine functionalised QDs with p.L and Smac. EDC activates the carboxylate groups present on the peptides and in the presence of the amine functionalised QDs, a covalent bond is formed.

3.11.3. Desalting of the bi-conjugates using gel filtration

The bi-conjugates prepared in **Section 3.7** were then subjected to desalting using the PD10 gel filtration column (GE Healthcare) as described in **Section 3.8.** The objective of this section was to determine which fraction contained the QD peptide bi-conjugate. This was determined by comparing the fluorescence intensities of the various elutes, as demonstrated in **Figure 3.3**.

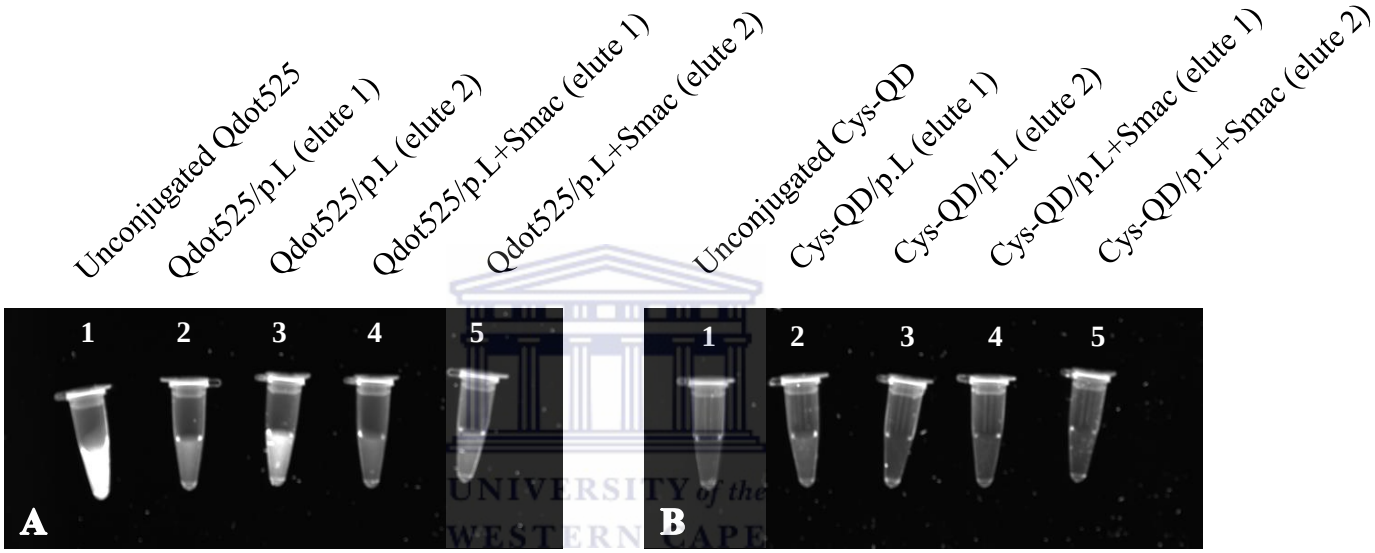

Figure 3.3. Desalted QD peptide bi-conjugates. In (A) Qdot525 peptide bi-conjugates and (B) Cys-QD peptide bi-conjugates, Lane 1 represent the unconjugated QDs. Lanes 2 and 3 represent elutes 1 and 2, respectively for the QD/p.L bi-conjugates. Lanes 4 and 5 represent elutes 1 and 2, respectively for the QD/p.L+Smac bi-conjugates. Images were captured using the UVP system.

The unconjugated Qdot525 sample showed the highest fluorescence. This was expected, since these QDs were in a more concentrated form. The Qdot525/p.L and Qdot525/p.L+Smac elute 2 had a higher fluorescence intensity than that of their elute 1 counterparts. This suggests that elute 2 contained most of the Qdot525 peptide bi-conjugates. The unconjugated Cys-QDs fluorescent signal was not as bright as that of the unconjugated Qdot525 sample. Contrary to the Qdot525 peptide bi-conjugates, the Cys-QD/p.L elute 1 had a higher

fluorescent signal than that of Cys-QD/p.L elute 2, suggesting that more of the Cys-QD peptide bi-conjugates were present in this fraction. Overall, the Cys-QD had a very poor fluorescent signal which may be accounted for by low concentrations (350 µg/ml) used in the bi-conjugation reactions. Nonetheless, the presence of a fluorescent signal in multiple fractions, confirmed the presence of the QDs, therefore, suggesting the presence of the QD peptide bi-conjugates. Based on the fluorescence intensities of the various fractions observed in **Figure 3.3**, elute 2 for the Qdot525 peptide bi-conjugates and elute 1 for the Cys-QD peptide bi-conjugates were used for further experiments.

3.11.4. Evaluating the cytotoxicity of the QD bi-conjugate targeted delivery system using the WST-1 Cell Proliferation assay

The objective of this section was to evaluate the cytotoxicity of (1) Qdot525/p.L+Smac and (2) Cys-QD/p.L+Smac by combinatorial treatment with ceramide. This was achieved by seeding and treating the cells as described in **Section 3.9.1 and 3.9.2.**

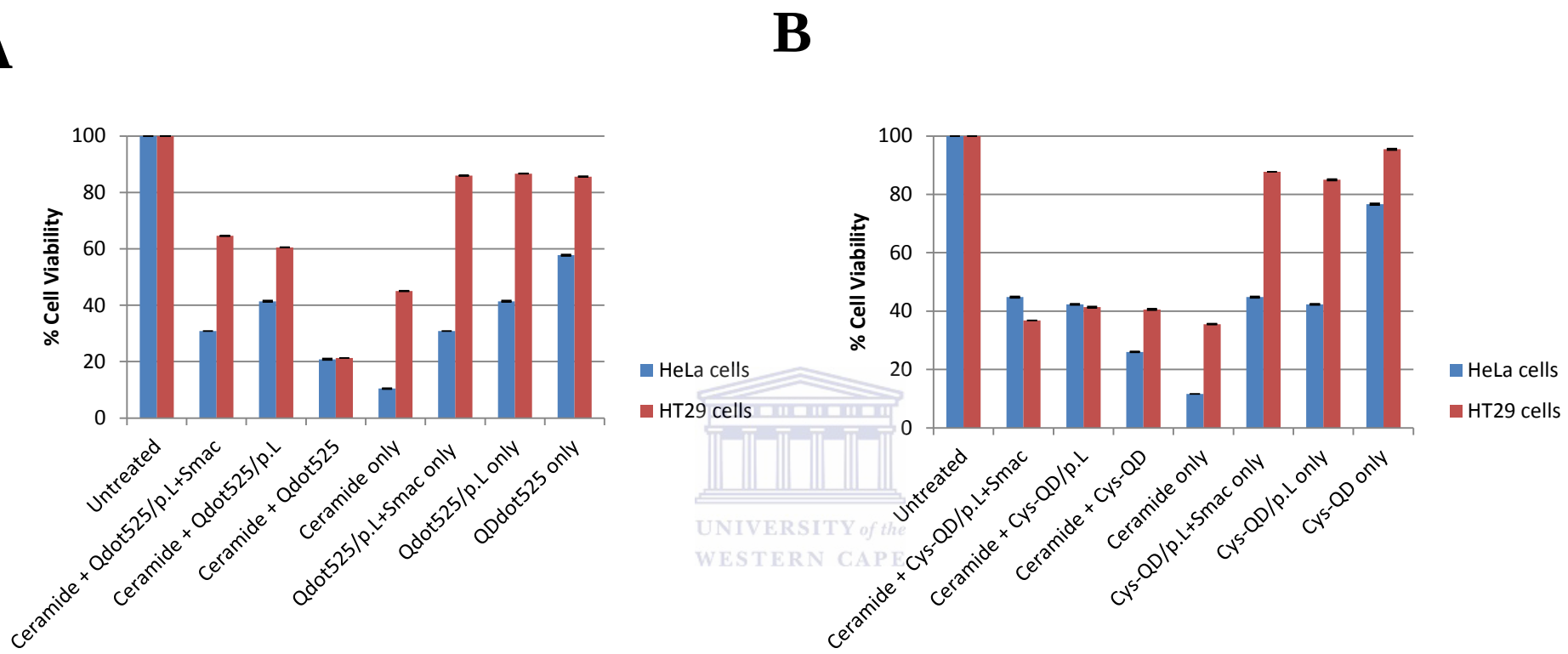

Figure 3.4. Evaluating the cytotoxicity of the targeted drug delivery system. HT29 and HeLa cells were subjected to treatment with the Qdot525 peptide bi-conjugate or the Cys-QD peptide bi-conjugate in the presence or absence of ceramide for 24 hrs. Subsequently, the cell viability was analysed using the WST-1 colometric assay. The data was obtained in triplicate and used to construct dose response curves for the respective QDs (mean ± SD; n=3). Error bars represent calculated standard error of the means.

Figure 3.4 shows the cytotoxic profile of the respective QD/p.L+Smac bi-conjugates. The Qdot525/p.L+Smac bi-conjugate did not enhance the apoptotic effect of ceramide. On the contrary, a degree of cytoprotection or anti-apoptotic effect was observed for HT29 cells as illustrated by the 20 % increase in cell viability conferred by the Qdot525/p.L+Smac bi-conjugate (65 % cell viability) as compared to the ceramide only control (45 % cell viability). It is possible that the Qdot525 peptide bi-conjugates interacted with ceramide and induced an inhibitory effect on ceramide induced apoptotic signalling because the Qdot525/p.L+Smac bi-conjugate failed to induce statistically significant cell death when treated without ceramide (86 % cell viability). The cytoprotective effect observed may also be due to insufficient concentrations of the Smac peptide. This may be as a result of a poorly controlled conjugation setup in that, there may have been competitive conjugation between the p.L and Smac peptides for the amine groups present on the QD surface, potentially resulting in insufficient quantities of the Smac peptide being conjugated to the QD peptide bi-conjugate. Smac has been reported to exert its inhibitory effects on XIAP by interaction with its BIR3 domain (Arnt *et al*., 2002 & Fandy *et al*., 2008), therefore, with the possibility that an insufficient concentration of Smac being used, may have resulted in suboptimal inhibitory action on XIAP; subsequently, low levels of caspase 3 displacement occurred and therefore, no synergistic anti-cancer activity was observed.

Under the same conditions, HeLa cells appear to be more susceptible to ceramide induced cell death (10 % cell viability) as compared to HT29 cells (45 % cell viability). However, again an inhibitory effect was observed when treated with the Qdot525/p.L+Smac bi-conjugates and ceramide (31 % cell viability). Therefore, suggesting that the Qdot525 targeted drug delivery system together with ceramide failed to induce a synergistic anti-cancer effect.

There were no statistically significant differences observed between the Cys-QD/p.L+Smac bi-conjugate (45 % cell viability) and the ceramide only control (36 % cell viability) for HT29 cells. Since the Cys-QDs surface chemistry is different from that of the Qdot525, in that there is no polymer coating, the potential interaction observed for the QD525/p.L+Smac bi-conjugate may be absent in Cys-QD/p.L+Smac bi-conjugate. Therefore, no cytoprotection was conferred in HT29 cells. Under the same conditions, HeLa cells showed more susceptibility to ceramide only induced cell death (12 % cell viability) as compared to HT29 cells (36 % cell viability). There were no statistically significant differences in the response of HeLa cells to the treatment with ceramide and the Qdot525/p.L+Smac bi-conjugate (31 % cell viability) as well as the Cys-QD/p.L+Smac bi-conjugate (45 % cell viability). The general observations for the HeLa cell line were greater susceptibly to cell death induced by the Qdot525/p.L+Smac and Cys-QD/p.L+Smac in the presence and absence of ceramide. This may be explained by the fact that a dose response trial was not carried out for HeLa cells and thus, the LD_{50} for this cell line may have been lower.

In a study carried out by Fandy *et al*., it was demonstrated that the level of IAP expression in various tumour types determines how the cancer cells will respond to the Smac peptide. The N-terminal Smac peptide was only able to sensitise low expressing IAP cancer cells; whereas it was able to induce apoptosis in high expressing IAP cancer cells (Fandy *et al*., 2008). Furthermore, Emjedi *et al*., showed that HT29 and HeLa cells are low expressing XIAP cell lines (Emjedi *et al*., 2013), therefore, it is possible that the expression level of IAPs in HT29 cells were insufficient to induce sensitising to apoptosis and consequently, no synergistic anti-cancer activity was observed. In this instance, the targeted drug delivery system developed in this study will prove to be ineffective.

Alternatively, it is known that the targeting function of the Smac peptide is elicited by the first four amino acids at its N-terminal (Wu *et al*., 2000 & Gao *et al*., 2007 & Martinez-Ruiz *et al*., 2008) and thus, the seemingly poorly controlled bi-conjugation setup in this study may have resulted in the bi-conjugation of the Smac peptide (N-terminal) to the p.L peptide (C-terminal), produced by EDC chemistry. The aim of using EDC chemistry was to exclude potential cross-reactivity by producing directly complexed QD peptide bi-conjugates (Herman, 2008); however, since EDC serves to complex any available carboxylic group to any available amine group, the possible peptide-peptide (p.L-Smac) product may have instigated an obstruction at the binding site of the Smac peptide, rendering Smac inactive. Therefore, the use of an alternative bi-conjugation scheme or the incorporation of a linker sequence (Fandy *et al*., 2008) may produce Qdot525/p.L+Smac or Cys-QD/p.L+Smac bi-conjugates that are able to enhance the ceramide induced cell death.

3.11.5. Evaluating the binding affinity of the QD peptide bi-conjugates

The objective of this section was to assess and compare the binding affinity of (1) the Qdot525 peptide bi-conjugates and (2) Cys-QD peptide bi-conjugates to HT29 and HeLa cells. To undertake this, HT29 and HeLa cells were cultured and seeded as described in **Section 3.5.1 and 3.5.3.** Since the QDs offer good fluorescent properties, the QDs were used to quantify the fluorescence intensity, indicative of the QD peptide bi-conjugate binding to the cells.

Figure 3.5 and 3.6 shows the binding of the Qdot525 peptide bi-conjugates and the Cys-QD peptide conjugates to HT29 and HeLa cells, respectively. There were no significant differences between the manner in which the unconjugated QDs and the respective QD

peptide bi-conjugates stained the cells. Firstly, this data suggests that the untargeted QDs are able to penetrate the cellular membrane, which is in agreement with Cho *et al*., who reports that the cellular uptake of free nanoparticles are attributed to their small size range and therefore permits internalisation of nanoparticles with great ease (Cho *et al*., 2008). Secondly, this data suggests that selective targeting was not achieved. EDC served to directly complex the QD peptide bi-conjugates (Herman, 2008); however, the results suggest that this may not have been an appropriate method of bi-conjugation.

The targeting function of the p.L peptide may have been elicited by its C-terminal and thus, the close proximity of the QDs to the p.L peptide, produced by EDC, may have resulted in the loss of the p.L peptide's ability to target the erbB-2 receptor. Therefore, the use of an alternative bi-conjugation scheme or the incorporation of a linker sequence may produce a bi-conjugate that is able to target efficiently. From the literature, very efficient targeting using the p.L peptide has been demonstrated; an example of this was reported by Jie *et al*, (2012) who used EDC bi-conjugation chemistry. However, to ensure more efficient targeting devoid of interference with the binding affinity and specificity, the p.L peptide was PEGylated (Jie *et al*., 2012).

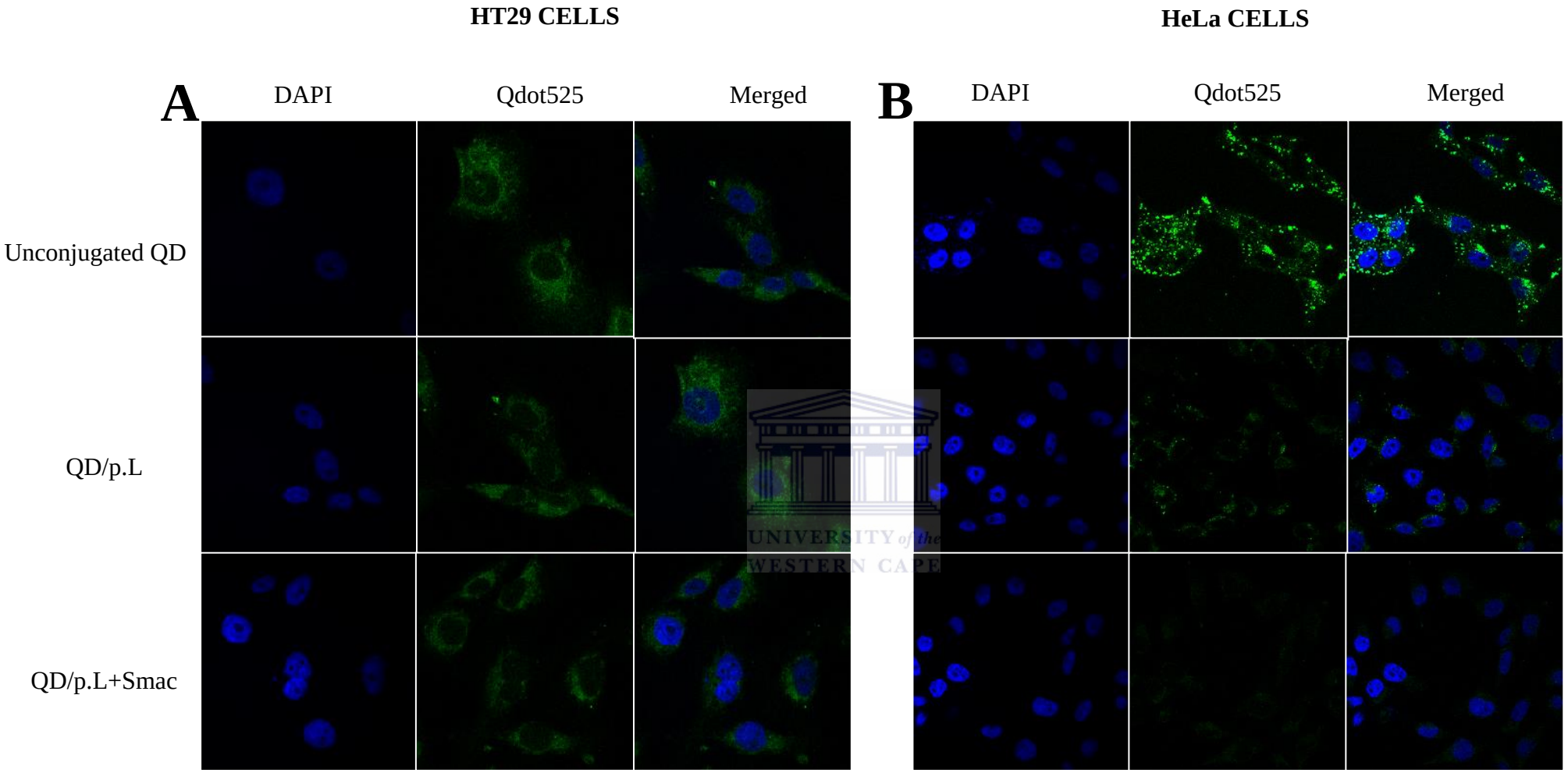

Figure 3.5. Binding of the Qdot525 peptide bi-conjugates. (A) HT29 and (B) HeLa cells were incubated with the respective Qdot525 peptide bi-conjugates for 1 hr and then counterstained with DAPI. Subsequently, the cells were examined under a confocal laser scanning microscope. Representative micrographs illustrate binding of the Qdot525 peptide bi-conjugates (green) and nuclei localisation (blue) in both cell lines. Images were captured at 100X magnification.

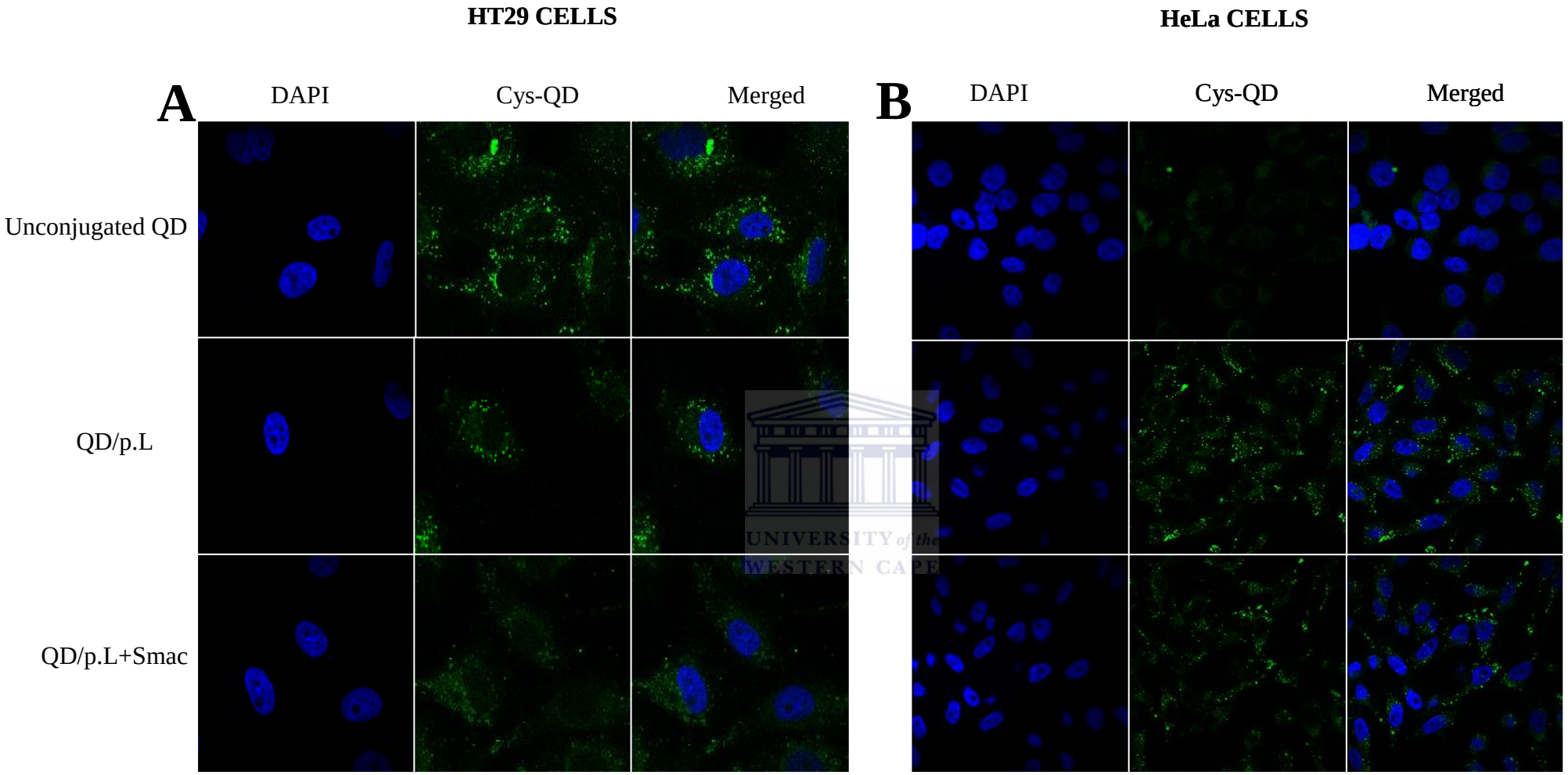

Figure 3.6. Binding of Cys-QD peptide bi-conjugates. (A) HT29 and (B) HeLa cells were incubated with the respective Cys-QD peptide bi-conjugates for 1 hr and then counterstained with DAPI. Subsequently, the cells were examined under a confocal laser scanning microscope. Representative micrographs illustrate binding of the Cys-QD peptide bi-conjugates (green) and nuclei localisation (blue) in both cell lines. Images were captured at 100X magnification.

Alternatively, the poor selectively presented by the p.L peptide in this study may be explained by the possibility that the bi-conjugation may have been unsuccessful. This would explain why there were no significant differences observed by the manner in which the unconjugated QDs and the QD peptide bi-conjugates stained the cells. Using tools such as PL spectroscopy and EDS, it may be possible to show that a successful bi-conjugation occurred. PL uses the principle of exposing the sample to light and the PL (emitted light) gets stimulated by a higher energy, producing an emission spectrum that may be analysed computationally (Seyhan, 2003). Any red shifted emissions from that of the unconjugated QDs would communicate an increase in the QD diameter and therefore, suggest the presence of the peptide on the QD surface and in turn, a successful bi-conjugation. EDS relies on the generation of a unique x-ray spectrum produced by the unique atomic structure ascribed to every element. Therefore, the presence of any biological materials in an elemental analysis by EDS would suggest the bi-conjugation of the QDs to the peptides.

3.11.6. Evaluating the internalisation of the bi-conjugates using live cell immunocytochemistry

The literature reports the p.L peptide being able to internalise erbB-2 positive breast cancer cells (Sioud and Mobergslien, 2012). Since HT29 cells have high expression levels of the erBb-2 receptor, the objective of this section is to determine whether the p.L peptide also internalises HT29 cells.

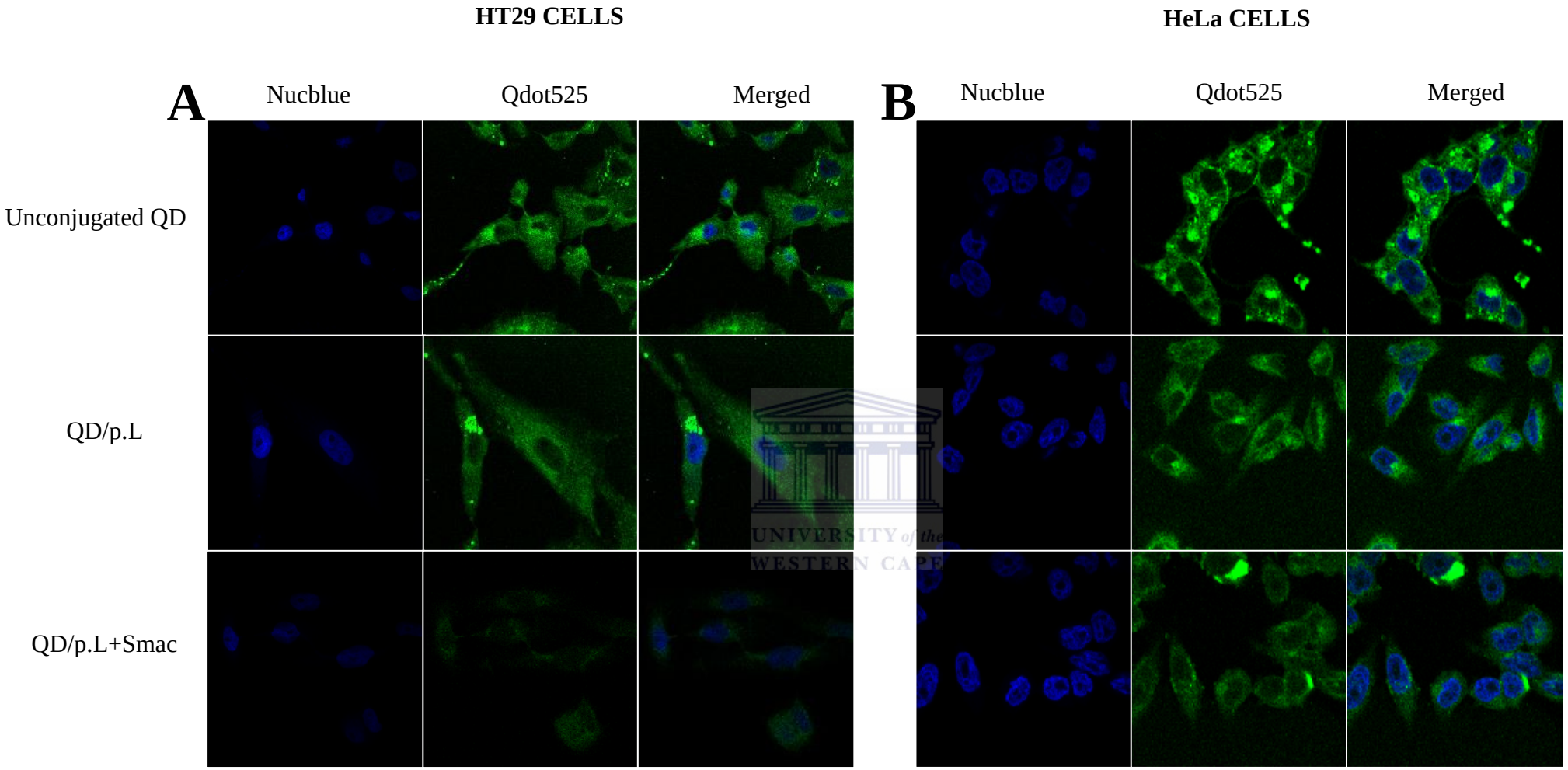

Figure 3.7. Internalisation of the Qdot525 peptide conjugates. (A) HT29 and (B) HeLa cells were incubated with the respective Qdot525 peptide bi-conjugates for 24 hrs and then counterstained with Nucblue. Subsequently, the cells were examined under a confocal laser scanning microscope. Representative micrographs illustrate efficient cellular uptake of the Qdot525 peptide bi-conjugates (green) and nuclei localisation (blue) in both cell lines. Images were captured at 100X magnification.

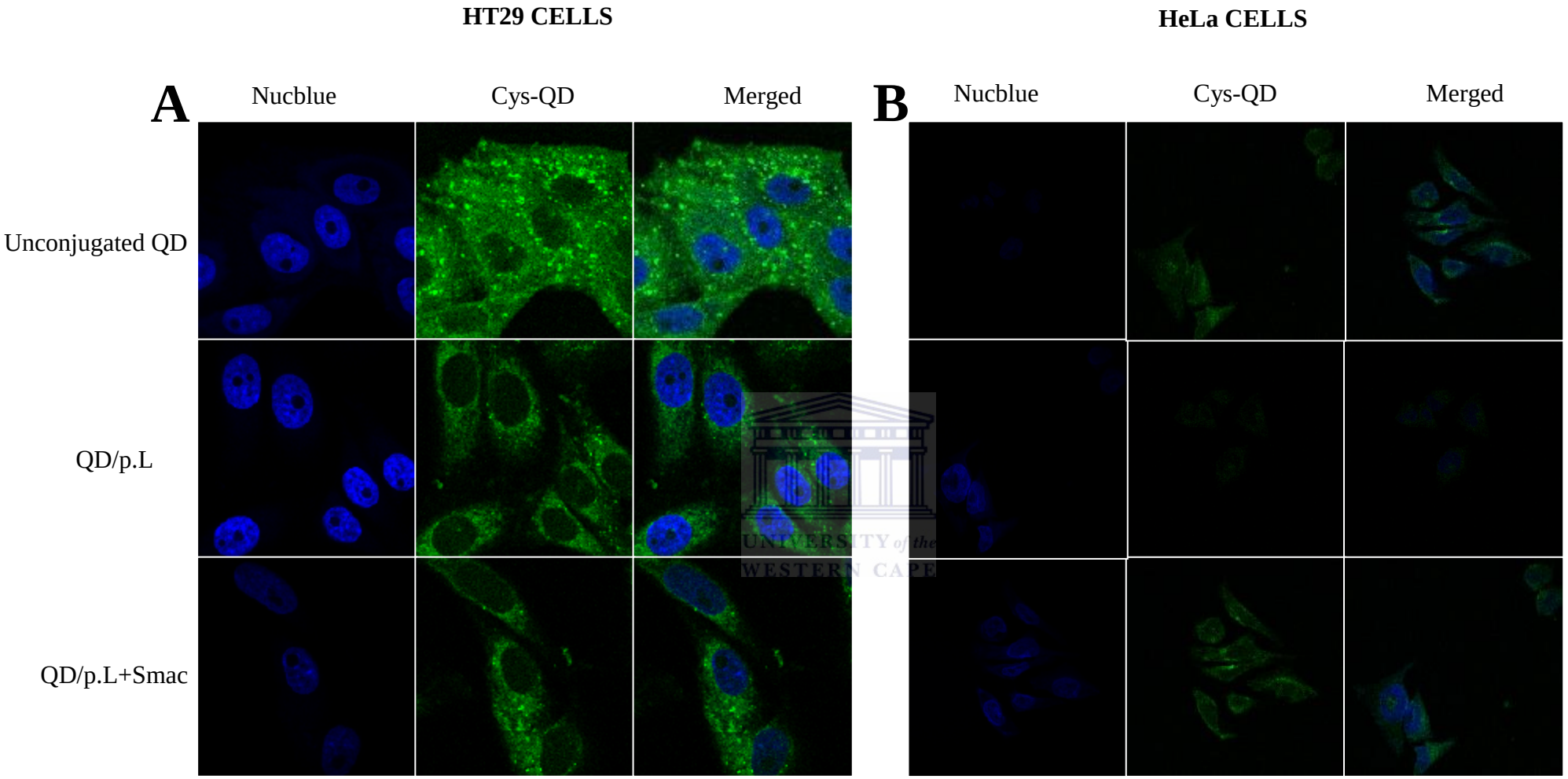

Figure 3.8. Internalisation of the Cys-QD peptide conjugates. (A) HT29 and (B) HeLa cells were incubated with the respective Cys-QD peptide bi-conjugates for 24 hrs and then counterstained with Nucblue. Subsequently, the cells were examined under a confocal laser scanning microscope. Representative micrographs illustrate efficient cellular uptake of the Cys-QD peptide bi-conjugates (green) and nuclei localisation (blue) in both cell lines. Images were captured at 100X magnification.

Figures 3.7 and 3.8 show the internalisation of the QD peptide bi-conjugates in HT29 and HeLa cells. There were no significant differences observed between the manner in which the unconjugated Qdot525 and the Qdot525 peptide bi-conjugates as well as the Cys-QD and Cys-QD peptide bi-conjugates stained the HT29 cells. This correlates with the fixed cell immunocytochemistry data (**Figure 3.5 and 3.6**) suggesting that selective targeting was not achieved. This may be due to an unsuccessful bi-conjugation, suggesting that what essentially is being observed is the staining of unconjugated QDs in all three instances (unconjugated QD or QD/p.L or QD/p.L-Smac) instead of the expected QD peptide bi-conjugates. Therefore, it would be advisable to establish whether the bi-conjugation in this study has been successful using the techniques previously discussed.

Of note, the Qdot525 peptide bi-conjugates were very efficiently taken up by HeLa cells as well. This may be explained by the reason that PEGylated QDs assists with escape from endosomal trapping (Choi *et al*., 2011) resulting in no difference in the manner in which the different cell lines internalised the Qdot525 peptide bi-conjugates due to PEGylation of the Qdot525. This in turn explains why the Cys-QD peptide bi-conjugates showed much higher fluorescence intensity in HT29 cells as compared to that of HeLa cells, indicative of very efficient internalisation to HT29 cells since the Cys-QDs were not synthesised with any polymer coating. To fairly evaluate the uptake of the QD peptide bi-conjugates developed in this study, QDs with the exact chemistry should be used.

The data from this section demonstrated efficient uptake of the QD peptide bi-conjugates, however, no selective targeting to HT29 cells were observed; this may be attributed to the previously discussed factors explained in **Section 3.11.5**. This data also corroborates results obtained for the cytotoxicity assay, in that the QD peptide bi-conjugates were not

successfully conjugated and therefore, no enhanced ceramide induced cell death was observed in the presence of the Qdot525/p.L+Smac or Cys-QD/p.L+Smac bi-conjugates and in fact, what was observed as no enhanced anti-cancer activity in **Figure 3.4** is representative of unconjugated QDs in each instance where the Qdot525/p.L+Smac or Cys-QD/p.L+Smac bi-conjugates were expected to be internalised.

Summary of this study

4.1. General Discussion

Cancer is a leading cause of death, worldwide. It is a progressive disease, in that accumulative changes occur at the genetic level. Subsequently, presenting a disease that is complex and life-threatening (Pal and Nayak, 2010). Annual projections are expected to reach approximately 16 million new mortality cases by 2020 (Thundimadathil, 2012). These statistics suggest that current therapeutic strategies appear to be less effective and therefore presenting a need for alternative therapeutic approaches (Sumer and Gao, 2008).

The non-specific distribution of conventional chemotherapeutic drugs, imposes severe toxicities, thereby restricting the drug dosages that may be administered (Wang *et al*., 2009). Overall, the objective is to produce an effective treatment, which directly targets and kills the cancerous cells, with little to no damage inflicted on healthy cells (Brannon-Peppas and Blanchette, 2004 & Byrne *et al*., 2008). In view of this, the therapeutic goal of chemotherapy has shifted towards targeted drug delivery systems; which have successfully been demonstrated using cancer specific peptides (Byrne *et al*., 2008 & Haglund *et al*., 2009 & Sioud and Mobergslien, 2012 & Thundimadathil, 2012). In particular, the p.L peptide that has been shown to successfully target several erbB-2 positive cancer cells (Shadidi and Sioud, 2002 & Shadidi and Sioud, 2003 & Wang *et al*., 2007 & Haglund *et al*., 2009 & Jie *et al*., 2012).

Additionally, the application of apoptosis inhibitory peptides as potential therapeutic modalities in targeted drug delivery systems have been reported (Shadidi and Sioud, 2003). Smac/DIABLO is a pro-apoptotic peptide that is able to interact with IAPs, thereby inducing pro-apoptotic signalling (Wu *et al*., 2000). It has been demonstrated in literature that

Smac/DIABLO and N-terminal Smac-derived short peptides enhance the anti-cancer activity of several drugs that induce apoptosis in cancer cells (Chai *et al*., 2000 & Arnt and Kaufmann, 2003 & Martinez-Ruiz *et al*., 2008 & Lu *et al*., 2011).

Nanotechnology has emerged as a promising avenue to formulate appropriate and efficient drug carriers for targeted drug delivery systems (Cao and Wang, 2011). Several nanoparticles have successfully been used in cancer treatment, of which QDs served as a delivery vehicle and imaging agent (Drbohlavova *et al*., 2009).

QDs are fluorescent semiconductor colloidal crystalline nanoparticles with diameters, generally, ranging between 2-10 nm in size (Chan *et al*., 1998 & Mattheakis *et al*., 2004) and are widely being applied as imaging agents (Resch-Genger *et al*., 2008). The unique properties exhibited by QDs are attributed to their physicochemical characteristics and therefore in the advent of synthesising these nanoparticles, determining what these characteristics are and how it plays a vital role in understanding its behaviour and subsequent application in biological systems (Zhang and Clapp, 2011).

The objective of this study was to develop a multimodal nanoparticle-based targeted drug system using peptide directed QDs as an imaging agent and delivery vehicle to selectively kill cancer cells using the pro-apoptotic peptide, Smac in combinatorial treatment with ceramide. To achieve this, highly monodispersed and green emitting fluorescent CdSe/ZnS core-shell QDs were synthesised using an organometallic approach. PL spectroscopy illustrated that the as prepared CdSe/ZnS core-shell QDs had a narrow and sharp PL spectrum, indicative of a narrow size distribution. Additionally, wavelength emissions at 525 nm were observed and therefore, suggesting green fluorescent QDs were obtained. High resolution TEM micrographs confirmed that monodispersed and spherical shaped QDs were synthesised, however, poor lattice fringes were observed, indicative of poor structural quality

QDs. The EDS analysis revealed that all four elements, Cd, Se, Zn and S were present in the as prepared QDs. The abovementioned data proved satisfactory to proceed with ligand exchange to solubilise the QDs for biological application. Water-soluble L-cysteine capped CdSe/ZnS core-shell QDs (Cys-QDs) were obtained using the method described by Carillo-Carrion *et al*., 2009. This was established by observing the well-dispersed QDs in the aqueous solution, indicative of a successful ligand exchange.

The in-house synthesised Cys-QDs and commercially available Qdot525, with similar chemistry, were used comparatively in the development of p.L peptide directed QDs functionalised with Smac. A non-hazardous dosage of the respective QDs was obtained using a dose response curve. Based on the response of HT29 cells to treatment with the QDs, it was decided to use a concentration below the LD_{50}, that is, 0.25 µM and 350 µg/ml for the Qdot525 and Cys-QDs, respectively. Using the aforementioned concentrations, the QDs were bi-conjugated to the p.L peptide and Smac peptide using EDC chemistry. This was followed by desalting the QD peptide bi-conjugates (Qdot525-p.L-Smac *or* Cys-QD-p.L-Smac) using PD10 gel filtration columns and the fractions with the highest fluorescence intensities were used for subsequent experiments. The potential cytotoxicity of the targeted drug delivery system developed in this study was then evaluated using the WST-1 Cell Proliferation assay. It was found that the combinatorial treatment of the Qdot525/p.L+Smac and the Cys-QD/p.L+Smac bi-conjugates did not enhance nor sensitise HT29 and HeLa cells to ceramide induced cell death. This may be explained by several factors, such as (1) insufficient concentration of Smac being used, resulting in suboptimal inhibitory action on XIAP or (2) a potential obstruction at the binding site of the Smac peptide possibly caused by bi-conjugating the peptides to each other or (3) the low expression levels of XIAP in these particular cell lines failed to sensitise the cells to apoptosis. This was confirmed when the binding affinity and internalisation of the QD peptide bi-conjugates were evaluated using

immunocytochemistry. No selective targeting to HT29 cells was observed, however, a degree of internalisation was achieved. Despite internalisation, there were no significant differences between the manner in which the respective QD peptide bi-conjugates were taken up by HT29 and HeLa cells. This was not anticipated since the literature reports that HT29 and HeLa cells retain high and low expression levels of the erbB-2 receptor, respectively (Kavanagh *et al*., 2009). It is possible that the p.L peptide lost functionality due to the method of bi-conjugation. Additionally, the bi-conjugation may have been unsuccessful and therefore, no targeting was observed due to the absence of the targeting moiety.

4.2. Conclusion

The objective of this study was to develop a multimodal nanoparticle-based targeted drug system using peptide directed QDs as an imaging agent and delivery vehicle to selectively kill cancer cells using the pro-apoptotic peptide, Smac in combinatorial treatment with ceramide. Green fluorescent CdSe/ZnS core-shell QDs were successfully synthesised and solubilised for its application in a biological environment. This study suggests that the bi-conjugation strategy may have been unsuccessful as demonstrated by no selective targeting to HT29 cells. Additionally, the possibility of an inappropriate bi-conjugation strategy resulted in the ineffective combinatorial treatment of the QD peptide bi-conjugate and consequently, HT29 cells were not sensitised to ceramide induced cell death. Although the overall objective was not met, the efficiency of the in-house synthesised Cys-QDs in comparison to the commercially available Qdot525 was observed to be of good quality and therefore, may potentially be used in other biological applications.

4.3. Future work

Future directions would aim to address limitations identified in this study. Over time, L-cysteine forms dimers and renders the QDs insoluble in aqueous medium, thus alternative water soluble capping ligands may be investigated to produce water-soluble QDs that are stable for longer. The literature clearly demonstrates the targeting ability and apoptotic sensitising of the p.L peptide and Smac peptide, respectively. Therefore, the ineffective target drug delivery system developed in this study suggests that an unsuccessful bi-conjugation occurred, therefore, exploring alternative bi-conjugation strategies, such as the incorporation of a linker sequence to avoid the potential loss of the peptide function may be investigated. Finally, the current targeted drug delivery system should be tested on cell lines with different

levels of XIAP expression to evaluate if the conditions under which this system was developed may prove to be effective.

4.4. References

1. Allen, T.M and Cullis, P.R. (2004) 'Drug delivery systems: entering the mainstream'. *Drug Discovery*, 303, 1818 – 1822.
2. Angell, J.J. (2011) 'Synthesis and characterisation of CdSe/ZnS core-shell quantum dots for increased quantum yield'. Masters' Thesis, California Polytechnic State University, San Luis Obispo.
3. Arnt, C.R., Chiorean, M.V., Heldebrandt, M.P., Gores, G.J and Kaufmann, S.H. (2002) 'Synthetic Smac/Diablo peptides enhance the effects of chemotherapeutic agents by binding XIAP and cIAP1 in situ'. *The Journal of Biological Chemistry*, 277 (46), 44236 – 44243.
4. Arnt, C.R and Kaufmann, S.H. (2003) 'The saintly side of Smac/Diablo: giving anticancer drug-induced apoptosis a boost'. *Cell Death and Differentiation*, 10, 1118 – 1120.
5. Boatman, E.M and Lisensky, G.C. (2005) 'A safer, easier, faster synthesis for CdSe uantum dots nanocrystals'. *Journal of Chemical Education*, 82 (11), 1697 – 1699.
6. Brannon-Peppa, L and Blanchette, J.O. (2004) 'Nanoparticle and targeted systems for cancer therapy.' *Advanced Drug Delivery Reviews*, 56, 1649 – 1659.
7. Byrne, J.D., Betancourt, T and Brannon-Peppa, L. (2008) 'Active targeting schemes for nanoparticles systems in cancer therapeutics.' *Advanced Drug Delivery Reviews*, 60, 1615 – 1626.
8. Chai, J., Du, C., Wu, J.W., Kyin, S., Wang, X and Shi, Y. (2000) 'Structural and biochemical basis of apoptotic activation by Smac/diablo'. *Nature*, 406, 855 – 862.
9. Chen, N., He, Y., Su, Y., Li, X., Huang, Q., Wang, H., Zhang, X., Tai, R and Fan, C. (2011) 'The cytotoxicity of cadmium-based quantum dots'. *Biomaterials*, 33(2012), 1238 – 1244.

10. Cho, K., Wang, K and Nie, S. (2008) 'Therapeutic nanoparticles for drug delivery in cancer.' *Clinical Cancer Research*, 14, 1310 – 1316.
11. Choi, Y., Kim, K., Hong, S., Kim, H., Kwon, Y.J and Song, R. (2011) 'Intracellular protein target detection by quantum dots optimized for live cell imaging'. *Bioconjugate Chemistry*, 22, 1576 – 1586.
12. Dabbousi, B.O., Rodriguez-Viejo, J., Mikulec, F.V., Heine, J.R., Mattoussi, H., Ober, R., Jensen, K.F and Bawendi, M.G. (1997) '(CdSe)ZnS core – shell quantum dots: synthesis and characterisation of a size series of highly luminescent nanocrystallites'. *The Journal of Physical Chemistry B*, 101, 9463 – 9475.
13. Danhier, F., Feron, O and Preat, V. (2010) 'To exploit the tumor microenvironment: Passive and active tumor targeting of nanocarriers for anti-cancer drug delivery.' *Journal of Controlled Released*, 148, 135 – 146.
14. De Barros, A.L.B., Tsourkas, A., Saboury, B., Cardoso, V.N and Alavi, A. (2012) 'Emerging role of radiolabeled nanoparticles as an effective diagnostic technique.' *EJNMMI Research*, 2(39), 1 – 5.
15. Deveraux, Q.L and Reed, J.C. (1999) 'IAP family proteins - suppressors of apoptosis'. *Genes and Development*, 13, 239 – 252.
16. Duckett, C.S. (2005) 'IAP proteins: sticking it to Smac'. *Biochemical Journal*, 385, e1 – e2.
17. Emjedi, Z., Meyer, M and Madiehe, A. (2013) 'Targeted delivery of embelin to cancer cells'. Masters' Thesis, University of the Western Cape, South Africa.
18. Fandy, T.E., Shankar, S and Srivastava, R.K. (2008) 'Smac/DIABLO enhances therapeutic potential of chemotherapeutic drugs and irradiation, and sensitises TRAIL-resistant breast cancer cells'. *Molecular Cancer*, 4(60), 1 – 10.

19. Felding-Habermann, B., O'Toole, T.E., Smith, J.W., Fransvea, E., Ruggeri, Z.M., Ginsberg, M.H., Hughes, P.E., Pampori, N., Shattil, S.J., Saven, A and Mueller, B.M. (2001) 'Integrin activation controls metastasis in human breast cancer'. *PNAS*, 98(4), 1853 – 1858.
20. Ferrari, M. (2005) 'Cancer Nanotechnology: Opportunities and Challenges'. *Nature Reviews*, 5, 161 – 171.
21. Fischer, U and Schulze-Osthoff, K. (2005) 'New approaches and therapeutics targeting apoptosis in disease'. *Pharmacological Reviews*, 57, 187 – 215.
22. Fulda, S and Debatin, K.M. (2006) 'Extrinsic versus intrinsic apoptosis pathways in anticancer chemotherapy'. *Oncogene*, 25, 4798.
23. Fulda, S. (2009) 'Inhibitors of apoptosis (IAP) proteins: Novel insights into the cancer-relevant targets for cell death induction'. *ACS Chemical Biology*, 4(7), 499 – 501.
24. Gao, Z., Tian, Y., Wang, J., Yin, Q., Wu, H., Li, Y and Jiang, X. (2007) 'A dimeric Smac/Diablo directly relieves caspase-3 inhibition by XIAP'. *The Journal of Biological Chemistry*, 282 (42), 30718 - 30727.
25. Gomes, A.S.O., Vieira, C.S., Almeida, D.B., Santos-Mallet, J.R., Menna-Barreto, R.F.S., Cesar, C.L and Feder, D. (2011) 'CdTe and CdSe quantum dots cytotoxicity: A comparative study on microorganisms'. *Sensors*, 11, 11664 – 11678.
26. Grabolle, M., Ziegler, J., Merkulov, A., Nann, T and Resch-Genger, U. (2008) 'Stability and fluorescence quantum yield of CdSe-ZnS quantum dots – influence of the thickness of ZnS shell'. *Annals of the New York Academy of Sciences*, 1130, 235 – 241.
27. Guo, F., Nimmanapalli, R., Paranawithana, S., Wittman, S., Griffin, D., Bali, P., O'Bryan, E., Fumero, C., Wang, H.G and Bhalla, K. (2002) 'Ectopic overexpression

of second mitochondria-derived activator of caspases (Smac/DIABLO) or cotreatment with N-terminus of Smac/DIABLO peptide potentiates epothilone B derivative-(BMS 247550) and APO-2L/TRAIL-induced apoptosis'. *Blood*, 99, 3419 – 3426.

28. Haglund, E., Seale-Goldsmith, M.M and Leary, J.F. (2009) 'Design of multifunctional nanomedical systems'. Annals of Biomedical Engineering, 1 – 16.
29. Hardman, R. (2006) 'A toxicological review of quantum dots: toxicity depends on physicochemical and environmental factors'. *Environmental Health Perspectives*, 114(2), 165 – 172.
30. Hermanson, G.T. (2008) *Bioconjugate Chemistry.* 2nd ed. London: Academic Press.
31. Hermanson, G.T. (2013) *Bioconjugate Chemistry.* 3rd ed. London: Academic Press.
32. Hines, M.A and Guyot-Sionnest, P. (1996) 'Synthesis and characterisation of strongly luminescing ZnS-capped CdSe nanocrystals'. *Journal of Physical Chemistry*, 100, 468 – 471.
33. Ho, Y.P and Leong, K.W. (2010) 'Quantum dots-based theranostics'. *Nanoscale*, 2(1), 60-68.
34. Huy, B.T., Seo, M.H., Lim, J.M., Shin, D.S and Lee, Y.I. (2011) 'A systematic study on preparing CdS quantum dots'. *Journal of the Korean Physical Society*, 59(5), 3293 – 3299.
35. Jamieson, T., Bahkshi, R., Petrova, D., Pocock, R., Imani, M and Seifalian, A.M. (2007) 'Biological applications of quantum dots'. *Biomaterials*, 28, 4717 – 4732.
36. Jaracz, S., Chen, J., Kuznetsova, L.V and Ojima, I. (2005) 'Recent advances in tumor –targeting anticancer drug conjugates'. *Bioorganic and Medicinal Chemistry*, 13(2005), 5043 – 5054.

37. Jones, M., Nedelkjovic, J., Ellingson, R.J., Nozik, A.J and Rumbles, G. (2003) 'Photoenhancement of luminescence in colloidal CdSe quantum dot solution'. *Journal of Physical Chemistry*, 107, 11346 – 11352.
38. Jie, L.Y., Cai, L.L., Wang, L.J., Ying, X.Y., Yu, R.S and Du, Y.Z. (2012) 'Actively targeted LTVSPWY peptide modified magnetic nanoparticles for tumor imaging'. *International Journal of Nanomedicine*, 7, 3981 – 3989.
39. Jin, S., Hu, Y., Gu, Z., Liu, L and Wu, H.C. (2011) 'Application of quantum dots in biological imaging'. *Journal of Nanomaterials*, 2011, 1 – 13.
40. Li, Z.L and Cho, C.H. (2012) 'Peptides as targeting probes against tumor vasculature for diagnosis and drug delivery'. *Journal of Translational Medicine*, 10, 1 – 9.
41. Li, J., Wu, D., Miao, Z and Zhang, Y. (2010) 'Preparation of quantum dots bioconjugates and their applications in bio-imaging'. *Current Pharmaceutical Biotechnology*, 11, 662 – 671.
42. Liu, W., Choi, H.S., Zimmer, J.P., Tanaka, E., Frangioni, J.V and Bawendi, M. (2007) 'Compact cysteine-coated CdSe(ZnCdS) quantum dots for in vivo applications'. *Journal of American Chemical Society*, 129, 14530 – 14531.
43. Lu, J., McEachern, D and Sun, H. (2011) 'Therapeutic potential and molecular mechanism of a novel, potent, nonpeptide, Smac mimetic SM-164 in combination with TRAIL for cancer treatment'. *Molecular Cancer Therapeutics*, 10, 902 – 914.
44. Lu, R.M., Chen, M.S., Chang, D.K., Chiu, C.Y., Lin, W.C., Yan, S.L., Wang, Y.P., Kuo, Y.S., Yeh, Y.S., Yeh, C.Y., Lo, A and Wu, H.C. (2013) 'Targeted drug delivery systems mediated by a novel peptide in breast cancer therapy and imaging'. *PLOS one*, 8(6), 1 – 3.

45. Martinez-Ruiz, G., Maldonado, V., Ceballos-Cancino, G., Grajeda, J.P.R and Melendez-Zajgla, J. (2008) 'Role of Smac/Diablo in cancer progression'. *Journal of Experimental and Clinical Cancer Research*, 27(48), 1 – 7.
46. Medintz, I.L., Uyeda, H.T., Goldman, E.R and Mattoussi, H. (2005) 'Quantum dot bioconjugates for imaging, labelling and sensing'. *Nature Materials*, 4, 435 – 446.
47. Nichols, J.W and Bae, Y.H. (2012) 'Odyssey of a cancer nanoparticle: From injection site to site of action'. *Nano Today*, 7, 606 – 618.
48. Normanno, N., De Luca, A., Bianco, C., Strizzi, L., Mancino, M., Maiello, M.R., Carotenuto, A., De Feo, G., Caponigro, F and Salomon, D, S. (2005) 'Epidermal growth factor receptor (EGFR) signalling in cancer'. *Gene*, 366(2006), 2 – 16.
49. Nguyen, K.T. (2011) 'Targeted nanoparticles for cancer therapy: promises and challenges.' *Journal of Nanomedicine and Nanotechnology*, 2(5), 1 – 2.
50. Oudhia, A. (2012) 'UV-Vis spectroscopy as a non-destructive and effective characterisation tool for II-VI compounds'. *Recent Research in Science and Technology*, 4(8), 109 – 111.
51. Pal, D and Nayak, A.M. (2010) 'Nanotechnology for targeted delivery in cancer therapeutics.' *International Journal of Pharmaceutical Sciences Review and Research*, 1(1), 1 – 7.
52. Pechstedt, K., Whittle, T., Baumberg, J and Melvin, T. (2010) 'Photoluminescence of colloidal CdSe/ZnS quantum dots: The critical effect of water molecules.' *Journal of Physical Chemistry*, 114, 12069 – 12077.
53. Pong, B.K., Trout, B.L and Lee, J.M. (2008) 'Modified ligand exchange for efficient solubilisation of CdSe/ZnS quantum dots in water: A procedure guided by computational studies'. *American Chemical Society*, 24, 5270 – 5276.

54. Qi, L., Colfen, H and Antonietti, M. (2000) 'Synthesis and characterisation of CdS nanoparticles stabilised by double-hydrophilic block copolymers'. *Nanoletters*, 1(2), 61 – 65.
55. Rajalingam, K., Oswald, M., Gottschalk, K and Rudel, T. (2007) 'Smac/Diablo is required for effector caspase activation during apoptosis in human cells'. *Apoptosis*, 12, 1503 – 1510.
56. Rao, C.N.R and Biswas, K. (2009) 'Characterisation of nanomaterials by physical methods'. *Annual Review of Analytical Chemistry*, 2, 435 – 462.
57. Reiss, P., Protiere, M and Li, L. (2009) 'Core/shell semiconductor nanocrystals'. *Small*, 5(2), 154 – 168.
58. Resch-Genger, U., Grabolle, M., Calaviere-Jaricot, S., Nitschke, R and Nann, T. (2008) 'Quantum dots versus organic dyes as fluorescent labels'. *Nature Methods*, 5 (9), 763 – 775.
59. Seyhan, A. (2003) 'Photoluminescence Spectroscopy of CdS and GaSe'. Masters' Thesis, The Graduate School of Natural and Applied Science of The Middle East Technical University, The Middle East.
60. Shadidi, M and Sioud, M. (2002) 'Identification of novel carrier peptides for the specific delivery of therapeutics into cancer cells'. *The FASEB Journal*, 1, 1 – 17.
61. Shadidi, M and Sioud, M. (2003) 'Selective targeting of cancer cells using synthetic peptides'. *Drug Resistance Updates*, 6(2003), 363 – 371.
62. Shiozaki, E.N and Shi, Y. (2004) Caspases, IAPs and Smac/Diablo: mechanisms from structural biology. '*TRENDS in Biochemical Sciences*', 39 (9), 486 – 494.
63. Singh, R and Lillard Jr, J.W. (2009) 'Nanoparticle-based targeted drug delivery'. *Experimental and Molecular Pathology*, 86(3), 215 – 223.

64. Sinha, R., Kim, G.J., Nie, S., shin, D.M. (2006) 'Nanotechnology in cancer therapeutics: bioconjugated nanoparticles for drug delivery'. *Molecular Cancer Therapeutics*, 5(8): 1909 – 1917.
65. Sioud and Mobergslien (2012) 'Selective killing of cancer cells by peptide-targeted delivery of an anti-microbial peptide'. *Biochemical Pharmacology*, 84(2012), 1123 – 1132.
66. Steichen, S.D, Caldorera-Moore, M. and Peppas, N.A. (2012) 'A review of current nanoparticle and targeting moieties for the delivery of cancer therapeutics'. *European Journal of Pharmaceutical Sciences*, 48(2013), 416 – 427.
67. Sumer, B and Gao, J. (2008) 'Theranostic medicine for cancer.' *Nanomedicine*, 3(2), 137 – 140.
68. Svensen, N., Walton, J.G.A. and Bradley, M. (2012) 'Peptides for cell-selective drug delivery'. *Trends in Pharmacological Sciences*, 33(4), 186 – 192.
69. Takeuchi, H., Kim, J and Fujimoto, A. (2005) 'X-linked inhibitor of apoptosis protein expression level in colorectal cancer is regulated by hepatocyte growth factor/c-met pathway via Akt signalling'. *Clinical Cancer Research*, 11, 7621 – 7628.
70. Tamm, I., Kornblau, S.M and Segall, H. (2000) 'Expression and prognostic significance of IAP-family genes in human cancers and myeloid leukemias'. *Clinical Cancer Research*, 6, 1796 – 1803.
71. Thundimadathil, J. (2012) 'Cancer treatment using peptides: Current therapies and future prospects'. *Journal of Amino Acids*, 2012, 1 – 13.
72. Tiwari, D.K., Tanaka, S.I., Inouye, Y., Yoshizawa, K., Watanabe, T.M and Jin, T. (2009) 'Synthesis and characterisation of anti-her2 antibody conjugated CdSe/ZnS quantum dots for fluorescence imaging of breast cancer cells.' *Sensors*, 9, 9332 – 9354.

73. Vashist, S.K. (2012) 'Comparison of 1-ethyl-3-(3dimethylaminopropyl) cardbodiimide based strategies to crosslink antibodies on amine-functionalised platforms for immunodiagnostic applications'. *Diagnostics*, 2, 23 – 33.
74. Vasir, J.K., Reddy, M.K., Labhasetwar, V.D. (2005) 'Nanosystems in drug targeting: Opportunities and challenges.' *Current Nanoscience*, 1, 47 – 64.
75. Wang, X.F., Witting, P.K., Salvatore, B.A and Neuzil, J. (2005) 'Vitamin E analogs triggers apoptosis in Her2/erbB2-overexpressing breast cancer cells by signalling via the mitochondrial pathway'. *Biochemical and Biophysical Research Communications*, 326(2005), 282 – 289.
76. Wang, X.F., Birringer, M and dong, L.F. (2007) 'A peptide conjugate of vitamin e succinate targets breast cancer cells with high erbB-2 expression'. *Cancer Research*, 67, 3337 – 3344.
77. Wang, X., Yang, L., Chen, Z and Shin, D.M. (2008) 'Application of nanotechnology in cancer therapy and imaging.' *A Cancer Journal for Clinicians*, 58, 97 – 110.
78. Wang, X., Wang, Y., Chen, Z.G and Shin, D.M. (2009) 'Advances of cancer therapy by nanotechnology'. *Cancer Research Treatment*, 41(1), 1 – 11.
79. Wei, Y., Fan, T and Yu, M. (2008) 'Inhibitor of apoptosis proteins and apoptosis'. *Acta Biochimica Biophysica Sinica*, 40 (4), 278 – 288.
80. Wilkinson, J.C., Wilkinson, A.S., Scott, F.L., Csomos, R.A., Salvesen, G.S and Duckett, C.S. (2004) 'Neutralisation of Smac/Diablo by inhibitors of apoptosis (IAPs): A caspase –independent mechanism for apoptotic inhibition'. *The Journal of Biological Chemistry*, 279 (49), 51082 – 51090.
81. Winnik, F.M and Maysinger, D. (2012) 'Quantum dots cytotoxicity and ways to reduce it'. *Accounts of Chemical Research*, 46(3), 672 – 680.

82. Wu, G., Chai, J., Suber, T.L., Wu, J.W., Du, C., Wang, X and Shi, Y. (2000) 'Structural basis of IAP recognition by Smac/Diablo'. *Nature*, 408, 1008 – 1012.

83. Xing, Y and Rao, J. (2008) 'Quantum dot bioconjugates for *in vitro* diagnostics & *in vivo* imaging'. *Cancer Biomarkers*, 4, 307 – 319.

84. Xu, H., Yu, Y and Marciniak, D. (2005) 'Epidermal growth factor receptor (EGFR)-related protein inhibits multiple members of the EGFR family in colon and breast cancer cells'. *Molecular Cancer Therapeutics*, 4, 435 – 442.

85. Yong, K.T., Ding, H., Roy, I., Law, W.C., Bergey, E.J., Maitra, A and Prasad, P.N. (2009) 'Imaging pancreatic cancer using bioconjugated InP quantum dots'. *ACS Nano*, 3 (3), 502 – 510.

86. Yu, M.K., Park, J and Jon, S. (2012) 'Targeting strategies for multifunctional nanoparticles in cancer imaging and therapy.' *Theranostics*, 2(1), 3 – 44.

87. Zhang, Y and Clapp, A. (2011) 'Overview of stabilising ligands for biocompatible quantum dot nanocrystals'. *Sensors*, 11, 11036 – 11055.

88. Zeng, R., Zhang, T., Liu, J., Hu, S., Wan, Q., Liu, X., Peng, Z and Zou, B. (2009) 'Aqueous synthesis of type II CdTe/CdSe core-shell quantum dots for fluorescent probe labelling tumor cells'. *Nanotechnology*, 20, 1 – 8.

89. Zhang, L., Gu, F.X., Chan, J.M., Wang, A.Z., Langer, R.S and Farokhzad, O.C. (2008) 'Nanoparticles in medicine: Therapeutic applications and developments'. *Clinical Pharmacology and Therapeutics*, 83 (5), 761 – 769.

90. Zou, Y., Li, D and Yang, D. (2010) 'Noninjection synthesis of CdS and alloyed CdS_xSe_{1-x} nanocrystals without nucleation initiators'. *Nanoscale Res Letters*, 5, 966 – 971.